

UDC 528.482

EVALUATION OF THE LOW-COST DEPTH CAMERAS FOR NON-DESTRUCTIVE TESTING

Noura Y. ALGHANIM¹, Tarig ALI¹, Ahmed ELAKSHER²✉, Mohammad ALHAMAYDEH¹

¹Civil Engineering Department, American University of Sharjah, Sharjah, UAE

²College of Engineering, New Mexico State University, Las Cruces, NM, USA

Article History:

- received 11 October 2023
- accepted 03 December 2024

Abstract. The primary aim of this paper is to assess the effectiveness of a low-cost stereo (depth) camera as a non-destructive tool for the detection and measurement of cracks in concrete surfaces. The experiment was carried out on four concrete beams with cracks, created with different concrete mixes. The mixes of the four beams were made up of lightweight aggregates with 12% of normal weight aggregates. One beam was used as a reference without fibers, while 3D steel fiber reinforcement, 5D steel fibers reinforcement, and a hybrid fibers mix of 5D steel fiber and synthetic were used for the other three beams. The cracks in the beams were measured manually followed by taking their stereo images with a ZED camera. The ZED images were processed to produce 3D models of the concrete surfaces, which are useful for crack measurement in a three-dimensional framework. The project results are particularly significant in the measurement of all three dimensions (length, width and depth), with less than a 10% error between the actual and the experimental procedure. Relatively, multiple differential approaches gave a less accurate result of a 15% error mainly due to syntax errors. Results suggest that the ZED depth camera is an effective tool for robust detection and measurement of cracks in concrete surfaces.

Keywords: stereo cameras, crack detection, non-destructive testing, 3D measurement.

✉Corresponding author. E-mail: elaksher@nmsu.edu

1. Introduction

Prior to delving into the crack detection methodologies, it is imperative to develop an understanding of the nature of the problem of crack formation and propagation in concrete structures. In fracture theory, cracks are assumed to inherently exist in hardened cement, paste, and mortar under common climate conditions (Wittmann, 1987). Typically, subsequent to the concrete hardening process, sedimentation takes place which causes water-filled pockets to fill up causing the formation of horizontal cracks as shown in Figures 1a and 1b. Time-dependent cracking mechanisms are common in concrete structures and dif-

fer in the transpiration and the consequent crack orientation. For example, the development of a time-dependent temperature gradient during the hydration phase causes thermal cracking. Furthermore, the curing of the concrete after demolding causes the formation of another form of minute cracks known as shrinkage cracks. These non-structural crack formation processes, however, are not typically detrimental to the structural integrity and functionality of concrete. Nonetheless, subjecting concrete to critical loads can cause the catastrophic propagation of crack regions. Nama et al. (2015) argued that cracking could propagate due to other structural provocateurs that include corrosion and sulphate attacks. Typically, the severity of the cracked region is assessed based on the width of the cracks, as follows in Table 1.

Table 1. Crack severity standards

Thin	<1 mm
Medium	1–2 mm
Wide	>2 mm

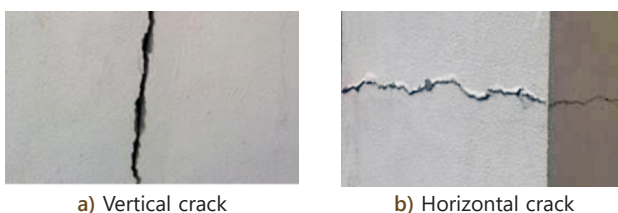


Figure 1. Cracks

Given the socioeconomic and operational complications that can arise from the dilapidation in the structural health of concrete due to cracking, it is imperative that progressive information on the wellbeing of the structure is documented in order to pre-emptively eschew such complications. The process of pre-emptive crack detection for concrete structural elements is a critical area in infrastructural quality assurance for the avoidance of the dilapidation of the structural integrity of concrete structures (Chong et al., 2003). Traditionally, cracks have been detected visually, which is a time-consuming and costly process. Visual inspection, according to Gholizadeh (2016), is the most basic and traditional form of NDT due to its technological simplicity and its primary reliance on labor utilization and procedural standardization. Davis (1998) argued that visual inspection relies on the experience of the investigators as well as their adherence to the rules and procedures outlined in certain guidebooks such as ACI 201.1R, ACI 207.3R, and, ACI 362R. Further, Davis (1998) explained the general approach to be adopted in visual inspection which starts with carrying out a cursory walk-through inspection for the investigator to familiarize with the structure being assessed. Then, a review of the relevant documentation of the project such as the design details, construction plans, and ambient conditions is necessary. Such method normally consists of a comprehensive assessment plan supported with visual inspection. In this case, the investigator needs to perform certain supplemental tests in order to ensure the reliability of the collected data and the results of the analysis.

In regards to the prospects and shortcomings of visual inspection, Verma et al. (2013) argued that the main benefit of visual inspections methods is their rapid data collection and low cost compared to technology-intensive methods. In a comparative study carried out by Agdas et al. (2015) to assess the cost of visual inspection and sensor-based inspection techniques, the cost of the sensor-based monitoring system for a coastal bridge, including equipment, labor, and miscellaneous hardware was estimated at \$29,000. On the other hand, the visual inspection process that was carried out for the same project incurred a total cost of \$11,900, taking into consideration the labor and equipment deployment costs. There are nonetheless certain disadvantageous associated with visual inspection that makes it unappealing in certain inspection scenarios. Verma et al. (2013) specifically stated that the reliance on the experience and subjective judgment of the investigator negatively affect the accuracy and reliability of the results attained through visual inspection. In an overview of the different image-processing-based techniques for crack detection, Mohan and Poobal (2017) showed that the main advantage of these techniques is their high accuracy relative to other methods.

While crack detection, which falls under the more comprehensive area of non-destructive testing (NDT), has been traditionally carried out through human inspection and assessment, the integration of smart technologies into NDT methodologies has introduced significant improvements

in the detection of deformations in the microstructures of concrete (Wang et al., 2020). As explained by Zhang et al. (2014) the parameters for effective crack detection involve three primary metrics which are detection rate, accuracy, and efficiency. Based on these metrics, recent trends in crack detection methodologies have relied on the automation of these non-destructive operations in order to reduce the margins of error and the costs that are typically associated with traditional manual inspection techniques (Le et al., 2017). In that sense, Milovanović and Pečur (2016) pointed out the diversity in innovation of automated NDT crack detection techniques that rely on frameworks such as visual and signal processing combined with the advancement in numerical algorithms. These frameworks have allowed for the effective identification of the cracks through remote sensing and detailed 3-D mapping techniques. Among the automated techniques that have attracted attention recently is the employment of depth cameras for the generation of detailed 3D maps of regions in concrete structures (Endres et al., 2014). This research aims at assessing the effectiveness of the proposed automated NDT technology for the detection of various crack patterns on concrete surfaces.

Mohan and Poobal (2017) have further presented an overview of the various image-based methodologies used for crack detection including camera-based, IR-based, and ultrasonic image processing. First, camera-based techniques assess the structural integrity of structural elements based solely on images. Sarker et al. (2017) developed an inexpensive depth camera crack detection system that was able to produce 3D model of the concrete surface. The high-resolution 3D imaging along with the point cloud created from it allowed for the generation of dense 3D dataset, which enabled for surface cracks detection even in low-lighting conditions. Similarly, Endres et al. (2014) developed an RGB-D camera system that was able to identify a variety of surface parameters in the crack area. Kim et al. (2017) fitted a hybrid image-processing unit on an Unmanned Ariel Vehicle (UAV) for crack-width estimation capabilities. The system hardware architecture also included an ultrasonic displacement sensor and a Wi-Fi communication link. Crack detection was carried out through image binarization and this system was successful in measuring thin cracks with an estimation error of 7.3%.

The IR-based method, on the other hand, utilizes thermal-IR cameras, which can identify the disparity in the temperature gradients between the cracks and the concrete surface. Milovanović and Pečur (2016) reviewed the technological trends in the use of IR-cameras for crack detection. In this case, thermal imaging can be carried out using passive or active thermal cameras. Passive IR cameras utilize emitted or reflected thermal energy by surfaces which is environmentally-friendly. Active thermal-IR cameras produce their own thermal energy in order to establish such a thermal gradient. Dumoulin et al. (2010) investigated the application of active infrared thermography for the detection of defects in rigid pavement (i.e. concrete pavement) and compared the results to that

estimated with a numerical simulations method (FLUENT). The results indicated the effectiveness of active thermography in fast and accurate defect identification. Xu et al. (2017) reached the same conclusion using a low-power piezoceramic transducer for the generation of thermal energy, but noted that the accuracy of the detection depend on the surface characteristics and the magnitude of used active-IR energy.

Ultrasound image-based methods involve the diffraction of ultrasound waves by crack regions on the concrete surface. Wiggerhauser and Niederleithinger (2013) presented an overview of some ultrasonic-based techniques that are capable of crack detection on concrete surface. These instruments included multi-offset array of ultrasonic transducers and embedded ultrasonic sensors in concrete structures. In a study by Pinto et al. (2010), it was found that ultrasound image processing with the time-of-flight diffraction would enable for crack depth estimation with an error of 10%.

Accordingly, NDT as defined by Helal et al. (2015) involves inspection, testing, and evaluation of materials and components without compromising the structural quality, serviceability or overall functionality of the part or the system. Furthermore, NDT encompasses a more panoptic set of methodologies that assess the integrity and quality of structures without affecting their reliability even if they involve invasive actions. In another study presented by Gholizadeh (2016), the author classifies the primary forms of NDT to include contact and non-contact testing. Contact testing requires contact between the sample specimen and the sensor, while non-contact testing can be done remotely. Table 2 provides a classification of the common contact and non-contact NDT methodologies.

Table 2. Common contact and non-contact NDT

Contact methods	Non-contact methods
Traditional ultrasonic testing	Through transmission ultrasonic
Eddy current	Radiography testing
Magnetic testing	Thermography
Electromagnetic	Infrared testing
Penetrant testing	Holography
Liquid penetrant	Shearography
Liquid penetrant	Visual inspection

For example, in cases that require the auto-detection of impact damage in carbon fiber composites, thermographic and radiographic testing is preferable. Alternatively, in cases that require the assessment of the dynamic characteristics for damage detection of structures, vibration methods are more adequate (Loutas et al., 2012). These considerations are important as it serves as a starting point for the optimization of the NDT operations. Given the direction of this study that focuses on non-contact methods of NDT, and based on the diversity in that class of NDT in itself, it is important to develop a general overview of the underlying principles of these methods and the latest

trends in their technologies. As aforementioned, the non-contact, or remote, methods of NDT are testing methods that do not require physical contact between the sensors and the concrete surfaces being assessed. Based on the information outlined in Table 2, it is clear that the majority of these methodologies require the integration of remote sensing and image fusion techniques. In fact, Morabito et al. (2008) argued that the utilization of the fusion techniques has been proved to yield superior results in the context of a single-sensor image modality. Nonetheless, it is essential to develop an understanding of some of the non-image-based non-contact NDT methodologies for the sake of comprehensiveness. Given the significance of crack detection and alleviation to the structural integrity of concrete structures, the primary objective of this project was the assessment of the feasibility and reliability of the use of a depth camera (ZED camera) for crack detection on concrete surfaces. This includes the development of an operational framework for the use of the depth camera as a tool for crack detection including image acquisition, image processing, 3D model creation, and cracks measurement. This study reviews the state of development of the image-based methods and their accuracy of crack detection and measurement, and further contributes to the literature through the assessment of the efficiency of a depth camera (ZED camera) for crack detection and measurement. A framework for using the ZED cameras for crack detection and measurement is developed and tested on concrete surfaces prepared with different mixes.

2. Methods

A framework for detection and measurement of cracks on concrete surfaces using a depth camera (ZED camera) is developed in this study. In order to evaluate the efficiency of this method it was applied to concrete surfaces prepared with different mixes. The concrete surfaces used in this study were for beams that have surficial cracks resulted due to the effect of normal-weight coarse-aggregate replacement by addition of fibers, and with steel fiber configuration without web reinforcement. The effect of these reinforcements on crack length, width and depth was assessed through conventional manual means and with the framework developed in this study. The framework consists of the following steps:

Stereo-image acquisition of the concrete surfaces using the ZED camera.

1. The 3D point cloud generation.
2. Development of 3D model of the cracks.
3. Decision on the condition of the surface based on the 3D measurement of the cracks (length, width, and depth), if any.

Stereo-image acquisition of the concrete surfaces using the ZED camera was carried out in this study using the ZED Explorer; a commercial software that comes with the camera. It was found out through experiments that placement of the ZED camera orthogonally at one-meter distance away from the concrete surfaces would help in

producing crack measurements. The resulted stereo images are then processed in the ZED Depth Viewer in order to create the depth map and the 3D point cloud of the crack area. Then 3D models of the cracks were created in the ZEDfu, a software that helped creating 3D mesh models of the cracks using the 3D point cloud data. Automatic crack detection on concrete surfaces was possible by applying gradient filter onto the mesh vertices. In order to visualize the detected cracks, color-coding representation was adopted. Then from the 3D mesh model, cracks lengths and widths were measured through digitizing. Cracks depths were then measured by slicing through the cracks in the 3D mesh models.

2.1. Experimental set-up

The experimental phase is the paramount part of this research project, which aimed to assess the functionality of the ZED camera in terms of crack detection and measurement. Accordingly, this article provides an overview of the general experimental set-up that was used in this study including tools and the concrete mix compositions, as well as a description of the procedures that were carried out to obtain the results of the experiment. A set of tools and components were deployed in order to carry out this experiment. First, the concrete specimens, which were used in this experiment, included four beams created from different mixes. Table 3 below outlines the composition of the four mixes.

Table 3. Concrete beam composition

Mix#	Composition
Mix#1	88% of lightweight aggregate with the addition of 12% normal weight aggregate in the mix
Mix#2	Mix#1 with the addition of 3D steel fibers reinforcement
Mix#3	Mix#1 with the addition of 5D steel fibers reinforcement
Mix#4	Mix#1 with the addition of hybrid fibers composite

In addition to the concrete beams with surface cracks, the following equipment and software were used in order to meet the objectives of this study. These include the following:

1. Standard measuring tape: the tape was used to manually measure the length and width of the visual cracks on the concrete surfaces.
2. ZED Stereo Camera: this camera (Figure 2) is a high-resolution 3D lightweight camera that has the specifications listed in Table 4. The ZED camera consists of two cameras, on the left and right, to provide a depth view, which can be used later to produce 3D models of the cracks through triangulation. This camera can acquire static or dynamic imagery.
3. ZED Explorer Software: this software enables for stereo image acquisition.

4. ZED Depth Viewer Software: this software is used for creating the depth map and the 3D point cloud for each imaged concrete surface. The 3D point cloud consists of thousands of georeferenced points.
5. ZEDfu Software: this software enables for creating 3D mesh models from the 3D point cloud. A mesh model is a 3D grid-like polygon.



Figure 2. ZED camera

Table 4. ZED camera specifications

Features	Specifications
Depth	0.5–20 m depth range
	32-bit depth format
	120 mm stereo baseline
Motion	6-axis pose accuracy
	100 Hz frequency
Lens	Filed view 90 (H) x 60 (V) x 110 (D)
	f/2.0 aperture
Sensors	4M pixels per sensor resolution
	native 16:9 sensor format

2.2. Experimental procedure

- The steps of the experimental procedure is illustrated in the workflow in Figure 4 below. Step [0]: Marking the grids on the surface of the beam.
- Step [1]: Defining the beam with its major crack regions (Figure 3). This involves the measurement of the crack length using a measuring tape.



Figure 3. Experimental setup of Mix#2 with defined cracks

- Step [2]: Place the ZED camera at a one-meter distance orthogonal to the concrete surface of the beam created with Mix#2. The image was then taken and exported to the ZED Explorer program (Figure 5).
- Step [3]: The images are then exported to the ZED Depth Viewer software in order to create depth map, and the 3D point cloud for Mix#2. The image is converted to tri-axis data and colorized in order to identify the cracks in the rendering software as shown in Figure 6. The image is then transformed to ZED explorer to generate a 3D point cloud image of the crack as shown in Figure 7.

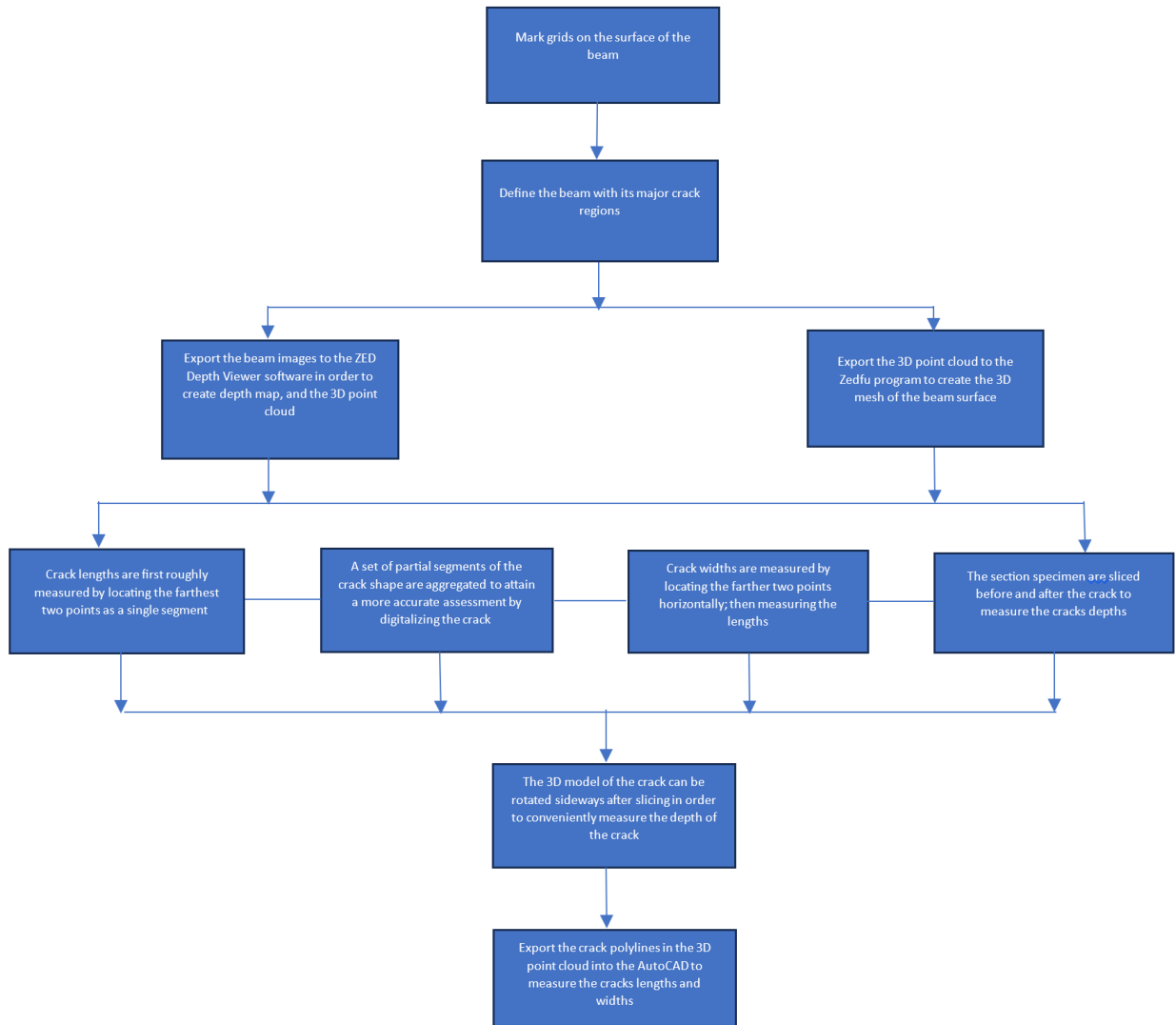


Figure 4. The workflow of the experimental procedure



Figure 5. ZED Explorer of Mix#2

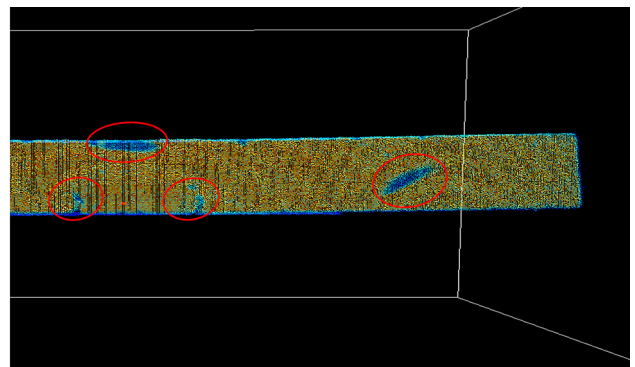


Figure 7. Point cloud Mix#2

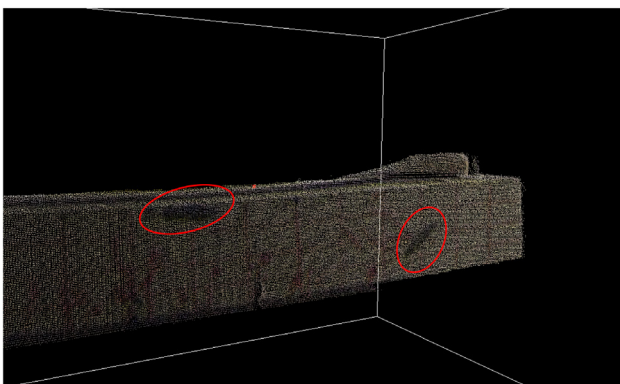


Figure 6. ZED Depth View of Mix#2

- Step [4]: The 3D point cloud is then exported to the ZEDfu program in order to create the 3D mesh of the surface as illustrated in Figure 8.
- Step [5]: The length is first roughly measured by locating the farthest two points a single segment (Figure 9).

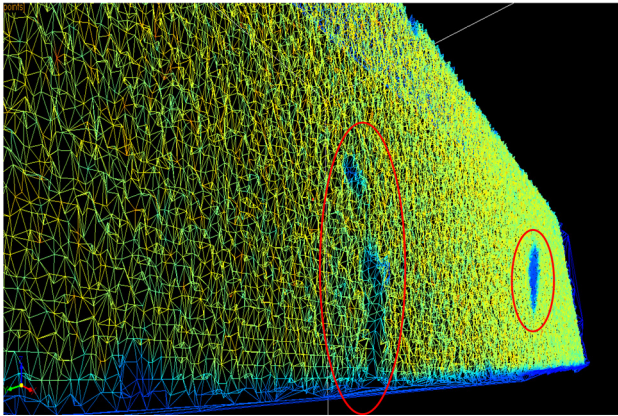


Figure 8. Mesh of Mix#2

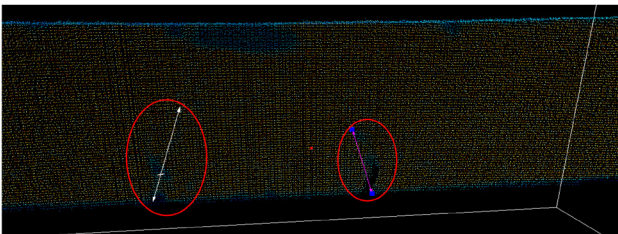


Figure 9. Defined points of Mix#2 for the single segment assessment

- Step [6]: A set of partial segments of the crack shape are aggregated to attain a more accurate assessment by digitalizing the crack. Ten segments were defined for this differential assessment (Figure 10). The selection of the points was based on locating localized regions around the crack. This is because the crack is a void, which requires locating regions within its proximity and relying on reasonable estimation. When the voids were too large, we used the surface model to allocate the points instead of the 3D mesh model in order to get location within the voids.

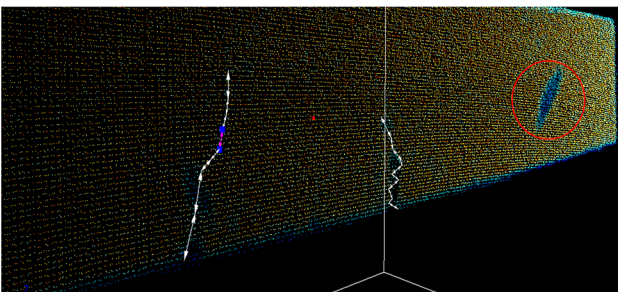


Figure 10. Defined points on Mix#2 for multiple segment assessment

- Step [7]: The width is measured by locating the farther two points horizontally; then measuring the length as can be seen in Figure 11.
- Step [8]: The section of the specimen was sliced immediately before and after the crack to measure the depth of the crack (Figure 12).

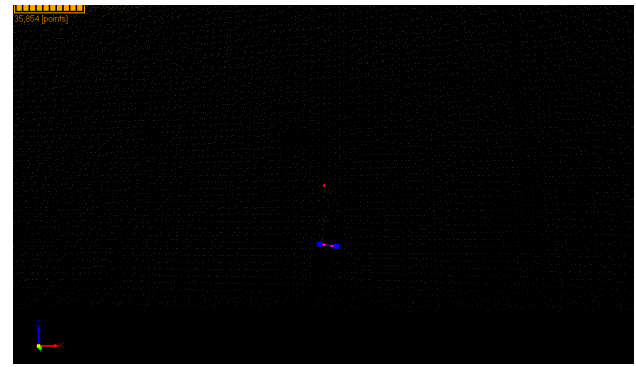


Figure 11. Width points of Mix#2

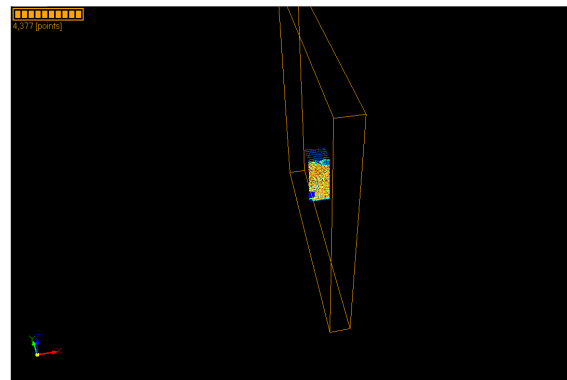


Figure 12. Sliced specimen of Mix#2

- Step [9]: The 3D model of the crack can be rotated sideways after slicing in order to conveniently measure the depth of the crack. The farthest points between the crack regions were chosen as shown in Figure 13. Then, the distance between the two points was measured by the taking perpendicular depth points. In some cases, it was difficult to locate points on the slice across the crack. In such cases, the slope was calculated.

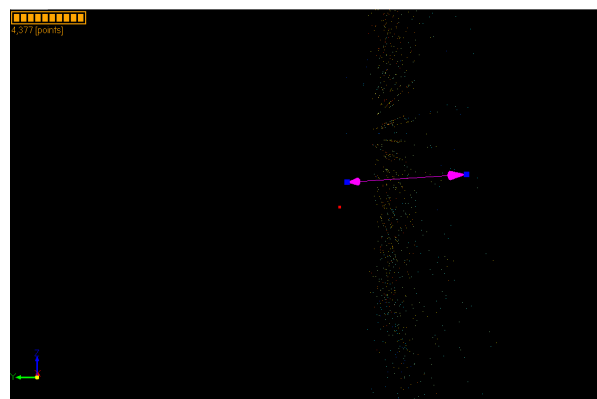


Figure 13. Perpendicular depth points of Mix#2

- Step [10]: Exporting the crack polylines in the 3D point cloud to the AutoCAD in order to measure the length and width of cracks as shown in Figure 14.
- Step [11]: Assessment of the accuracy of the crack measurements with ZED camera.

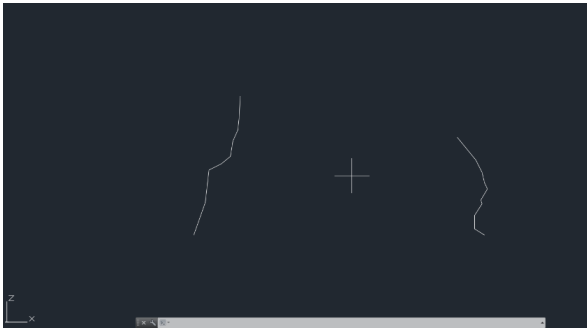


Figure 14. Crack polylines on AutoCAD for Mix#2

3. Results and discussion

The results were analyzed in order to assess the accuracy of the measurement for each of the four mixes. Table 5 below summarizes the measurements of the four mixes including the actual lab length (measured manually with a tape) and the method developed in this study using the ZED camera. These measurements are based on the farthest points on the cracks.

Table 5. One-segment measurements

Mix	Actual Length (cm)	ZED Experimental Length (cm)	*% Error
1	40.0	42.0	5.00%
2	L1 = 11.2	L1 = 11.8	5.36%
	L2 = 8.1	L2 = 8.3	2.47%
3	54.0	57.2	5.93%
4	41.0	41.3	0.73%

Note: *% Error = [(ZED measurement-Actual Length)/Actual Length].

The second sets of results are for the lengths measurements obtained for cracks polylines (multiple linear segments). Table 6 summarizes the results of using actual lab measurements, while Table 7 summarizes the measurements taken by the ZED camera. Table 8 reports the accuracy of the two procedures.

Table 6. Actual 10-segment lab measurements

Segments	Mix 1	Mix 2		Mix 3	Mix 4
		L1	L2		
1	11.1	2.0	1.5	13.2	4.0
2	8.2	1.5	1.8	12.0	3.0
3	5.4	1.5	1.5	5.0	8.0
4	1.8	1.2	1.0	2.9	5.7
5	6.9	1.3	1.4	1.0	3.9
6	6.1	2.0	1.0	2.1	1.4
7	4.0	1.0	1.4	2.0	4.7
8	1.2	1.4	1.0	5.0	1.0
9	3.4	1.4	0.8	4.2	1.8
10	2.4	2.2	1.3	1.6	4.5
Total L (cm)	50.5	15.5	12.6	50.3	38.0

Table 7. ZED experimental 10-segment lab measurements

Mix	Actual Length (cm)	ZED Experimental Length (cm)	*% Error
1	50.5	45.4	-10.10%
2	L1 = 15	L1 = 12.8	-14.67%
	L2 = 12.6	L2 = 10.8	-14.29%
3	50.3	57.7	14.71%
4	38.0	42.2	11.05%

Note: *% Error = [(ZED measurement-Actual Length)/Actual Length]

Table 8. 10-segment measurements accuracy error

Segments	Mix 1	Mix 2		Mix 3	Mix 4
		L1	L2		
1	11.1	2.0	1.5	13.2	4.0
2	8.2	1.5	1.8	12.0	3.0
3	5.4	1.5	1.5	5.0	8.0
4	1.8	1.2	1.0	2.9	5.7
5	6.9	1.3	1.4	1.0	3.9
6	6.1	2.0	1.0	2.1	1.4
7	4.0	1.0	1.4	2.0	4.7
8	1.2	1.4	1.0	5.0	1.0
9	3.4	1.4	0.8	4.2	1.8
10	2.4	2.2	1.3	1.6	4.5
Total L (cm)	50.5	15.5	12.6	50.3	38.0

The third set of results illustrates the measurements of the (widest) widths of cracks in the four specimens as shown in Table 9.

Table 9. Width measurements

Mix	Actual width (mm)	ZED experimental width (mm)	% Error
1	10.5	11.1	5.7%
2	L1 = 1.1	L1 = 1.2	9.0%
	L2 = 0.8	L2 = 0.72	10.0%
3	6.2	6.8	9.7%
4	7	7.4	5.7%

Then, the depths were measured in the 3D cracks models for the 4 mixes. The results of these measurements are summarized in Table 10.

Table 10. Depth measurements

Mix	ZED Depth (cm)
1	0.5
2	0.08
3	1.3
4	1.15

First, in terms of measuring the cracks lengths, the one segment approach does not give accurate lengths relative to the differential approach of multiple segments. In this approach, the crack is considered as a single continuous

segment, and the crack's length is calculated by simply measuring the distance between the two endpoints of this segment. This can be done by detecting the crack's edges and approximating the crack's length based on the endpoints of the detected feature. If the crack is curved or has a jagged shape, using a single segment might lead to significant inaccuracies. The length might be underestimated or overestimated because the method ignores the detailed geometry of the crack. These results are similar to the findings of Deng and Nakanishi (2011), who found that the use of a grid-pattern measurement is more effective in identifying the changes in cracks' lengths, which mitigate the margin of errors. The measurement of one linear segment of the crack, however, was necessary for calibrating the ZED camera.

Secondly, the pixilation quality of the computer program also plays an important role when it comes to measuring very small segments of cracks. The ability of the 3D point cloud mapping to pinpoint the exact localized beginning and ending points of the cracks makes the ZED-based approach more accurate relative to the manual measurement. This is mainly due to syntax errors that can emerge when relying on manual measurements (Zhang et al., 2014).

Nonetheless, another noteworthy observation in regards to the accuracy of the ZED camera is based on the environmental influence on its usability. Zhou et al. (2017) pointed to the superior usability of stereo cameras, such as the ZED, for thin structure assessment in large outdoor environments. Although the measurements have been made indoors, the study has examined a single object and the results cannot be extended to the measurement of indoor environments, which also conforms to the hypothesis presented by Sarkar et al. (2017).

Finally, it is important to point out that this image-based methodology could not be completely in an automated way because the ZED camera doesn't do all the work by itself. Firstly, experiments need photography experience in order to take quality stereo images of the concrete surfaces that have the cracks. Furthermore, familiarity with the associated software programs including ZED Depth Viewer and ZEDfu is important. These considerations need to be taken into perspective as future efforts in automatic crack detection and structural health monitoring.

Our results show that the ZED camera has capabilities that can be applied to crack identification and measurement. In the following sections, we will summarize our findings in this regards.

Ability of the ZED camera to identify cracks:

The ZED camera uses stereo vision, which allows it to capture depth information alongside standard RGB imagery. This can help with detecting cracks as variations in texture or surface discontinuities. By analyzing depth data, the camera can also distinguish surface irregularities that indicate cracks. However, crack identification can be challenging if cracks are very fine or if the surface is reflective or textured in a way that obscures the crack's edges. Environmental conditions (such as lighting) may also affect the performance of

crack detection algorithms. Shape and orientation of the cracks are typically estimated with good precision, as the ZED camera captures both visual and depth data, allowing for detailed analysis of crack morphology.

Accuracy of crack length measurement:

The ZED camera's stereo vision provides depth perception, which can help in measuring the length of visible cracks more accurately. With appropriate software, the camera can map out the dimensions of the crack based on the 3D point cloud data it generates. On the other hand, the accuracy of crack length measurement depends on factors such as the resolution of the camera, the scale of the crack, and how well the crack is captured in the camera's field of view. A crack that is too small or too far from the camera may result in less accurate measurements.

The accuracy of crack length measurement depends on the camera's resolution and the depth information. Long cracks that are clearly visible in the camera's field of view can be accurately measured, but very fine or subtle cracks may be harder to detect. The **semi-major axis** of the error ellipse usually runs along the crack's length (in the direction of the crack), where the uncertainty is more significant. The **semi-minor axis** may run perpendicular to the crack and represents the uncertainty in estimating the crack's boundary along its width.

Accuracy of crack width measurement:

The ZED camera are able to estimate the width of cracks by utilizing the disparity between the two camera images. This can be particularly useful for measuring crack widths in a relatively accurate manner, especially if the crack is well-defined and perpendicular to the camera view. But the accuracy can drop if the crack is not well-aligned to the camera's view, or if the crack's edges are not clear. Small cracks may also be harder to measure accurately if the camera's resolution isn't high enough for detailed analysis.

The measurement's accuracy is influenced by how well the crack is captured in the camera's depth map. If the crack is perpendicular to the camera's line of sight, it is easier to measure accurately. The precision can decrease with smaller cracks or if the crack is at an angle relative to the camera. The **semi-major axis** may align with the direction of greatest uncertainty, which is typically the perpendicular direction to the camera's view (or the crack's orientation). The **semi-minor axis** typically corresponds to the uncertainty in the horizontal (depth) direction, which usually has smaller effects in width measurement.

Accuracy of crack depth measurement:

The ZED camera's depth-sensing capability allows it to estimate the depth of cracks by analyzing the 3D data it generates. This can be valuable for cracks that are deep or have varying depths along their length. Yet, depth measurement accuracy depends on the disparity map's resolution, the distance between the crack and the camera, and the geometry of the crack. The ZED camera typically performs best when objects are relatively close and within a clear line of sight. Large cracks or those with complex geometries may pose challenges.

The depth measurement accuracy can vary with the resolution of the depth map, the distance from the camera, and the crack's geometric properties. Larger, more clearly defined cracks allow for better depth estimation than smaller or more complex cracks. The **semi-major axis** typically points along the depth direction, which represents the uncertainty in measuring how deep the crack is relative to the camera's position. The **semi-minor axis** corresponds to errors in lateral dimensions (length or width), but these are usually less pronounced than depth-related errors.

4. Conclusions

The experimental results obtained in this study conformed to previous research conducted in the area of crack detection and measurements on concrete surfaces. In that sense, the use of the ZED camera has provided more accurate and reliable results relative to manual measurements. The use of the ZED proved effective even in small, indoor environments. This is mainly due to the intrinsic functionality of the associated 3D point cloud program that allows for the measurement of crack dimensions (length, width, and depth) from localized points. The reliability is further substantiated by the proximity in the different attained dimensions. Furthermore, it is recommended that the usability of the ZED camera be handed to specialized operators who are able to attain high-quality stereo images of the crack regions on the concrete surface. This plays an important role as far as the processing of the computer-generated images due to pixilation and orientation concerns. Finally, familiarity with the use of the different software listed in this project plays an important role in the optimization of the overall process and ensuring the accuracy of the results.

There are certain inherent limitations in the project that compromised the efficiency of the overall project, which may be generally confronted as hardships to the replication of this project. For one, carrying out this project requires the utilization of a set of programs including ZED Depth Viewer, ZED Explorer, and ZEDfu. Thus, researchers need to ensure that all these programs are available to fulfill the objective of this project. While the ZED-based programs tend to come together as a package, the absence of one of them may compromise the fulfillment of the project objective. When calibrating the ZED camera measurements, it's important that the same points that mark the crack lengths are selected when performing the measurement manually (with the tape) and when using the ZED camera method.

The project outcomes are particularly significant in substantiating the usability of ZED camera for crack detection and measurement including all three dimensions (length, width and depth). Future work will focus on the full automaton of this process through the alleviation of the crack detection process in the 3D point cloud imaging phase and the centralization of the capturing, transfer, and processing of the images. This optimization can

improve the efficiency of the process in terms of accuracy, reliability, and timeliness, all of which are important variables in this project.

References

- Agdas, D., Rice, J., Martinez, J., & Lasa, I. (2015). Comparison of visual inspection and structural-health monitoring as bridge condition assessment methods. *Journal of Performance of Constructed Facilities*, 30(3), 1–21. [https://doi.org/10.1061/\(ASCE\)CF.1943-5509.0000802](https://doi.org/10.1061/(ASCE)CF.1943-5509.0000802)
- Chong, K. P., Carino, N. J., & Washer, G. (2003). Health monitoring of civil infrastructures. *Smart Materials and Structures*, 12(3), 483–493. <https://doi.org/10.1088/0964-1726/12/3/320>
- Davis, A. (1998). *Nondestructive test methods for evaluation of concrete in structures*. ACI Committee.
- Deng, G., & Nakanishi, T. (2011). Practical methods for crack length measurement and fatigue crack initiation detection using ion-sputtered film and crack growth characteristics in glass and ceramics. In C. Sikalidis (Ed.), *Advances in ceramics*. InTechOpen. <https://doi.org/10.5772/22594>
- Dumoulin, J., Ibos, L., Ibarra-Castanedo, C., Mazioud, A., Marchetti, M., Maldague, X., & Bendada, A. (2010). Active infrared thermography applied to defect detection and characterization on asphalt pavement samples: Comparison between experiments and numerical simulations. *Journal of Modern Optics*, 57(18), 1759–1769. <https://doi.org/10.1080/09500340.2010.522738>
- Endres, F., Hess, J., Sturm, J., Cremers, D., & Burgard, W. (2014). 3-D mapping with an RGB-D camera. *IEEE Transactions on Robotics*, 30(1), 177–187. <https://doi.org/10.1109/TRO.2013.2279412>
- Gholizadeh, S. (2016). A review of non-destructive testing methods of composite materials. *Procedia Structural Integrity*, 1(1), 50–57. <https://doi.org/10.1016/j.prostr.2016.02.008>
- Helal, J., Sofi, M., & Mendis, P. (2015). Non-destructive testing of concrete: A review of methods. *Electronic Journal of Structural Engineering*, 14(1), 97–105. <https://doi.org/10.56748/ejse.141931>
- Kim, H., Lee, J., Ahn, E., Cho, S., Shin, M., & Sim, S. (2017). Concrete crack identification using a UAV incorporating hybrid image processing. *Sensors*, 17(9), 20–52. <https://doi.org/10.3390/s17092052>
- Le, T., Gibb, S., Pham, N., La, H. M., Falk, L., & Berendsen, T. (2017). Autonomous robotic system using non-destructive evaluation methods for bridge deck inspection. In *2017 IEEE International Conference on Robotics and Automation (ICRA)* (pp. 3672–3677). IEEE. <https://doi.org/10.1109/ICRA.2017.7989421>
- Loutas, T., Panopoulou, A., Roulias, D., & Kostopoulos, V. (2012). Intelligent health monitoring of aerospace composite structures based on dynamic strain measurements. *Expert Systems with Applications*, 39(9), 8412–8422. <https://doi.org/10.1016/j.eswa.2012.01.179>
- Milovanović, B., & Pečur, I. B. (2016). Review of active IR thermography for detection and characterization of defects in reinforced concrete. *Journal of Imaging*, 2(2), Article 11. <https://doi.org/10.3390/jimaging2020011>
- Mohan, A., & Poobal, S. (2017). Crack detection using image processing: A critical review and analysis. *Alexandria Engineering Journal*, 57(2), 787–798. <https://doi.org/10.1016/j.aej.2017.01.020>
- Morabito, F., Simon, G., & Cacciola, M. (2008). Image fusion techniques for non-destructive testing and remote sensing applications. In *Image fusion* (pp. 367–392). Elsevier. <https://doi.org/10.1016/B978-0-12-372529-5.00013-5>

- Nama, P., Jain, A., Srivastava, R., & Bhatia, Y. (2015). Study on causes of cracks & its preventive measures in concrete structures. *International Journal of Engineering Research and Applications*, 5(5), 119–123.
- Sarker, M., Ali, T., Abdelfatah, A., Yehia, S., & Elaksher, A. (2017). A cost-effective method for crack detection and measurement on concrete surface. *International Archives of the Photogrammetry, Remote Sensing and Spatial Information Sciences, XLII-2/W8*, 237–241.
<https://doi.org/10.5194/isprs-archives-XLII-2-W8-237-2017>
- Verma, S., Bhadauria, S., & Akhtar, S. (2013). Review of nondestructive testing methods for condition monitoring of concrete structures. *Journal of Construction Engineering*, 2013, Article 834572. <https://doi.org/10.1155/2013/834572>
- Wang, B., Zhong, S., Lee, T. L., Fancey, K. S., & Mi, J. (2020). Non-destructive testing and evaluation of composite materials/structures: A state-of-the-art review. *Advances in Mechanical Engineering*, 12(4), 1–28.
<https://doi.org/10.1177/1687814020913761>
- Wiggenhause, H., & Niederleithinger, E. (2013). Innovative ultrasonic techniques for inspection and monitoring of large concrete structures. *EPJ Web of Conferences*, 56(4), 1–9.
<https://doi.org/10.1051/epjconf/20135604004>
- Wittmann, F. (1987). Structure of concrete and crack formation. In K. P. Herrmann & L. H. Larsson (Eds.), *Fracture of non-metallic materials* (pp. 309–340). Springer.
https://doi.org/10.1007/978-94-009-4784-9_15
- Xu, C., Xie, J., Zhang, W., Kong, Q., Chen, G., & Song, G. (2017). Experimental investigation on the detection of multiple surface cracks using vibrothermography with a low-power piezoceramic actuator. *Sensors*, 17(12), Article 2705.
<https://doi.org/10.3390/s17122705>
- Zhang, W., Zhang, Z., Qi, D., & Li, Y. (2014). Automatic crack detection and classification method for subway tunnel safety monitoring. *Sensors*, 14(10), 19307–19328.
<https://doi.org/10.3390/s141019307>
- Zhou, C., Yang, J., Zhao, C., & Hua, G. (2017). Fast, accurate thin-structure obstacle detection for autonomous mobile robots. In *2017 IEEE Conference on Computer Vision and Pattern Recognition Workshops (CVPRW)* (pp. 318–327). IEEE.
<https://doi.org/10.1109/CVPRW.2017.45>